Received: 1 November 2024 | Revised: 11 August 2025 | Accepted: 17 August 2025

DOI: 10.1111/bph.70189

RESEARCH ARTICLE

Optochemical modulation of corneal cold nerve terminal impulse activity with a photochromic ion channel blocker

David Ares-Suárez[1,2] | Almudena Iñigo-Portugués[1] | Enrique Velasco[1] | Susana Quirce[1] | Fernando Aleixandre-Carrera[1] | Ariadna Díaz-Tahoces[1] | M. Carmen Acosta[1] | Wan-Chen Lin[3] | Richard H. Kramer[3] | Carlos Belmonte[1] | Juana Gallar[1,2] | Victor Meseguer[1]

[1]Instituto de Neurociencias, Universidad Miguel Hernández–CSIC, Sant Joan d'Alacant, Spain

[2]Instituto de Investigación Sanitaria y Biomédica de Alicante, Alicante, Spain

[3]Department of Molecular and Cell Biology, University of California, Berkeley, California, USA

Correspondence
Victor Meseguer, Instituto de Neurociencias, Universidad Miguel Hernández–CSIC, Sant Joan d'Alacant, Spain.
Email: vmeseguer@umh.es

Funding information
MICIU/AEI, Grant/Award Numbers: RTI2018-100994-AI00, PID2021-124460OB-I00, PID2023-147915OB-I00; Conselleria de Cultura, Educación y Ciencia, Generalitat Valenciana, Grant/Award Number: CIPROM/2021/48

Background and Purpose: The functional organization of corneal cold nerve endings, critical structures in maintaining the ocular surface, remains poorly understood. Here, the photoisomerizable small-molecule diethylamine-azobenzene-quaternary ammonium (DENAQ) was used to photomodulate activity of cold-sensing nerve terminals in control and chronic tear-deficient corneas. Furthermore, DENAQ was used for in vivo photochemical regulation of the thermally induced blink reflex.

Experimental Approach: Extracellular nerve terminal impulse activity was recorded on cold terminals in excised corneas of naïve and tear-deficient guinea pigs pre-incubated with DENAQ. Pulses of light at a wavelength of 460 nm were delivered to the perfused corneas. The thermally induced blink reflex was assessed using orbicularis oculi electromyography in anaesthetised rats after topical administration of DENAQ to the eye under blue light and darkness conditions.

Key Results: Exposure to blue light robustly reduced spontaneous activity of both naïve and tear-deficient cold nerve terminals pre-incubated with DENAQ, while cold-evoked responses remained unaffected. Pre-incubation of excised corneas with DENAQ, along with pharmacological P2X receptor antagonists, prevented the DENAQ-mediated photoreduction of the cold nerve terminal spontaneous activity. In addition, blue light increased cold-evoked reflex blink in eyes pre-treated with DENAQ.

Conclusion and Implications: DENAQ enters guinea pig cold sensory nerve endings primarily through P2X channels in excised corneas. Subsequently, DENAQ decreases the spontaneous nerve terminal impulse activity upon light irradiation by modulating voltage-gated potassium (K_V) channel activity. Furthermore, the cold-evoked blink reflex is modulated by light in DENAQ-treated eyes. Chemical photoswitches like

Abbreviations: AUC, area under the curve; DENAQ, diethylamine-azobenzene-quaternary ammonium; DRG, dorsal root ganglion; EYFP, enhanced yellow fluorescent protein; HCN, hyperpolarization-activated cyclic nucleotide-gated (channels); K_V, voltage-gated potassium (channels); NTI, nerve terminal impulse; OOemg, orbicularis oculi electromyography; TEA, tetraethylammonium; TG, trigeminal ganglion.

DENAQ might be potential new treatments for ocular discomfort and pain in dry eye disease.

KEYWORDS
chemical photoswitches, cornea cold nerve endings, DENAQ, dry eye, ocular discomfort, P2X channels, voltage-gated potassium channels

1 | INTRODUCTION

Corneal cold receptors are peripheral axons of trigeminal ganglion (TG) neurons that are specialized for the sensory transduction of cold temperatures. Their ability to detect cooling of the ocular surface relies on the expression of **TRPM8** ion channels, which are activated by small temperature drops and osmolarity changes (González-González et al., 2017; Parra et al., 2010, 2014; Quallo et al., 2015). Both stimuli occur naturally under dry environments due to tear evaporation (Hirata & Meng, 2010; Purslow & Wolffsohn, 2007). Subsequently, action potentials from stimulated cold thermoreceptors propagate to higher order brainstem neurons (Belmonte et al., 2017; Marfurt, 1981; Pozo & Cervero, 1993). These neurons reflexively regulate tear flow and blinking rate (Parra et al., 2010; Quallo et al., 2015). Additionally, the information transmitted to the somatosensory cortex elicits conscious sensations of cooling or dryness, depending on the extent of the temperature reduction (Belmonte et al., 2017; Moulton et al., 2012). Dry eye, a common ocular disease associated with ageing, causes discomfort and unpleasant sensations of dryness as its primary symptoms (Vehof et al., 2013). In a chronic tear-deficient guinea pig model, corneal cold sensory endings exhibit increased excitability due to functional changes in sodium and potassium voltage-gated channels (Kovács et al., 2016).

Photoisomerizable small molecules, also known as photoswitches, can modulate neural activity by interacting with native ion channels without requiring exogenous gene expression. DENAQ, a synthetic photochromic blocker of ion channel (Mourot et al., 2011), confers light sensitivity to mouse retinal ganglion cells as well as binaural auditory gerbil neurons (Ko et al., 2016; Tochitsky et al., 2014, 2016). However, it remains unknown whether DENAQ can modulate the electrical activity of neural structures located far from the neuron cell body, such as corneal sensory nerve endings.

The cornea is a transparent and structurally simple tissue. Its nerve axons end a few μm below the epithelial surface, allowing for direct electrophysiological recording of identified nerve endings. This activity can be remotely controlled with light (Aleixandre-Carrera et al., 2021). Therefore, we selected this tissue as a model for combining treatment with DENAQ and electrophysiological approaches in guinea pig corneal cold sensory nerve endings.

A better understanding of the functional organization of the membrane channels of cold sensory nerve endings is necessary due to the crucial role that cold thermoreceptors play in the physiological and pathological states of the ocular surface. Previous studies have shown that **P2X** receptors mediate photoswitch entry to degenerated retinal ganglion cells in a mouse model of retinitis pigmentosa. Once inside the cell, DENAQ targets voltage-gated potassium (K_V) and hyperpolarization-activated cyclic nucleotide-gated (**HCN**) ion channels, which allows light to control the firing of action potentials in these cells (Tochitsky et al., 2014, 2016). Based on this, we hypothesized that DENAQ-mediated photosensitivity could act as a highly sensitive reporter for the functional expression of P2X ion channels in peripheral nerve endings, including corneal cold sensory endings.

Here, using animal models, we have found that DENAQ primarily enters corneal cold sensory nerve endings through P2X ion channels. This compound produced, in the presence of light, a robust decrease of the spontaneous electrical activity of the cold nerve terminals, in both control and pathological conditions such as chronic tear deficiency. Also, we demonstrated the ability of DENAQ to photomodulate the cold-evoked blink reflex after its topical instillation onto the eye.

What is already known

- The activity of corneal cold nerve endings is essential for maintaining ocular surface health.
- Photoisomerizable molecule DENAQ permeates P2X7 ion channels, conferring light sensitivity to mouse retinal ganglion cells.

What does this study add

- DENAQ enters the cold-sensitive nerve endings of guinea pig corneas primarily through P2X3 ion channels.
- DENAQ photomodulates corneal cold nerve activity under blue light in guinea pig and rat models.

What is the clinical significance

- Topical DENAQ may help reduce the increased activity of corneal sensory nerve terminals following injury.
- Photoswitches such as DENAQ might be potential new treatments for dry eye disease.

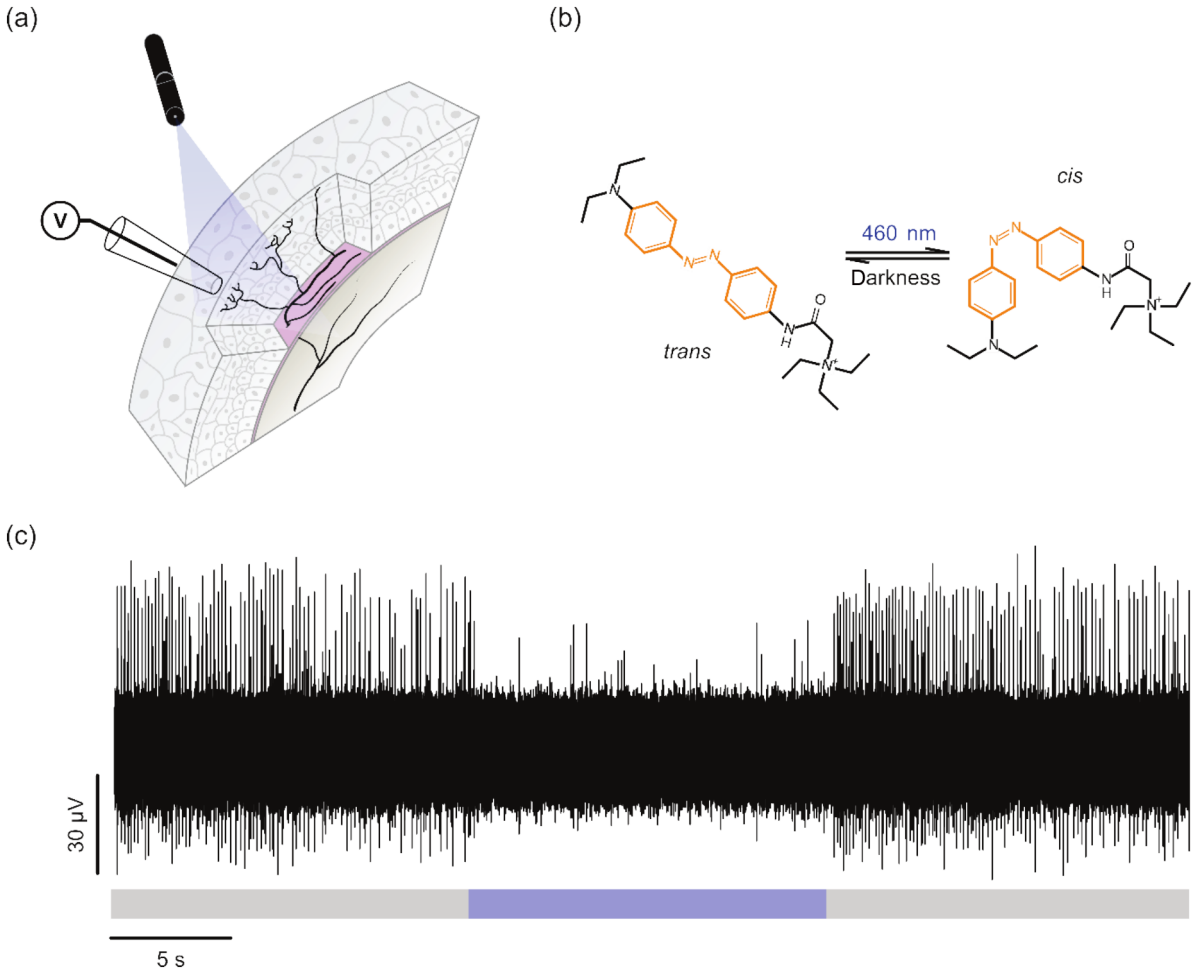

FIGURE 1 (a) Illustration of the electrophysiological extracellular recording of nerve terminal impulses (NTIs) at excised guinea pig corneas. An LED-emitting light of 460 nm of wavelength was applied. (b) Chemical structure of DENAQ in *trans* (darkness) and *cis* conformation (light). The light-sensitive component of DENAQ, azobenzene, is highlighted in orange. (c) Example of the spontaneous NTI activity recorded at a constant temperature of 34°C in a guinea pig corneal cold-sensitive nerve terminal in darkness (grey bars) and under light irradiation (blue bar).

2 | METHODS

2.1 | Experimental animals

All animal care and experimental procedures followed the National Institutes of Health (NIH) Guide for the Care and Use of Laboratory Animals, the European Union Directive (2010/63/EU), and the Spanish regulations on the protection of animals used for experimentation and scientific purposes. The protocol was approved by the Committee on Ethics and Integrity in Research of the University Miguel Hernández. All animals were randomly assigned to the experimental groups. Animal studies are reported in compliance with the ARRIVE guidelines (Percie du Sert et al., 2020) and with the recommendations made by the *British Journal of Pharmacology* (Lilley et al., 2020).

Dunkin Hartley guinea pigs (Envigo RMS Spain SL, Barcelona, Spain) of both sexes were used at 2-3 months, transgenic TRPM8^{BAC}-EYFP mice of both sexes (institutional animal facility, Instituto de Neurociencias, San Juan de Alicante, Spain) (Morenilla-Palao et al., 2014) were used at 3-6 months, and Wistar rats (Harlan Laboratories SA, Barcelona, Spain) were used at the age of 4 months old (2 female/1 male; not intended to compare by sexes). The animals were kept in individual cages, maintained in a 12-h light/dark cycle, and housed in a temperature-controlled (23 ± 2 °C) and humidity-controlled (55 ± 10 %) facility with food and water available ad libitum.

2.2 | Corneal nerve terminal electrophysiological recordings

Corneas were prepared for electrophysiological recordings following the protocol described by Acosta et al. (2013). The corneas were cut circularly at the limbus using iris scissors and then gently placed in a beaker with a physiological solution. The solution had a composition of 133.4-mM NaCl, 4.7-mM KCl, 2-mM $CaCl_2$, 1.2-mM $MgCl_2$, 16.3-mM $NaHCO_3$, 1.3-mM NaH_2PO_4 and 9.8-mM glucose, with an osmolarity of 310 mOsm·L^{-1}, and bubbled with carbogen (95% O_2 and 5% CO_2) for 60 min to maintain pH at 7.4. The corneas were cut into two equal pieces and then incubated with DENAQ at 200 µM or

2 mM for 40 min at 34°C. Next, each piece of cornea was placed in a perfusion chamber, fixed and secured with insect pins to the silicone at the bottom of the chamber (Sylgard 184; Dow Corning, Midland, MI, USA). Extracellular recording of nerve terminal impulses (NTIs) was used to detect the activity of corneal cold thermoreceptors. This was achieved by applying a 50-µm-diameter glass micropipette onto the corneal surface under gentle suction, as described by Brock et al. (1998) (Figure 1a). A maximum of one nerve terminal was recorded from each piece of cornea. The corneas were continuously superfused with the physiological solution at a 2.5-ml·min^{-1} flow during the electrophysiological recording. The bath solution temperature was kept at 34°C (basal temperature) using a feedback-regulated, homemade Peltier device. Cold ramps were applied to 15°C using a Peltier device. The recording electrode, made of Ag, was placed inside the glass micropipette. Electrical signals were recorded relative to an Ag/AgCl pellet placed in the chamber. The electrical activity was amplified by a factor of 100 using the NL 103 AC amplifier (Digitimer, Welwyn, UK). The signal was then filtered using the NL 125/NL 126 filter from Digitimer, with a high-pass filter of 5 Hz and a low-pass filter of 5 kHz. The filtered signal was stored in a computer at a 20-kHz rate using a CED interface and Spike2 software. Only NTIs originating from single cold-sensitive terminals were selected for further study. They were identified by their relatively high level of regular spontaneous discharge, occasionally in bursts, that increased prominently with cooling. The ongoing NTI activity at the basal temperature was recorded for at least 100 s before applying the light stimulation protocol.

2.3 | Chronic tear-deficiency model

Chronic tear deficiency is commonly used as an animal model of dry eye disease. Tear deficiency is induced by excising the main lacrimal gland on the left and right sides (Kovács et al., 2016). Guinea pigs were anaesthetised with ketamine (90 mg·kg^{-1} i.p.) and xylazine (5 mg·kg^{-1} i.p.). An 8-mm skin incision was then made on the temporal side, posterior to the lateral canthus, over the fibrous capsule of the exorbital gland to access the main lacrimal gland, which was then gently excised. The surgical site was inspected to confirm the complete removal of all remaining glandular tissue. An antibiotic drop (tobramycin, 3 mg·ml^{-1}) was applied to the surgical site to prevent infection and promote animal welfare. Finally, the skin incision was sutured with a 6.0 braided silk suture. Animals were individually housed for 1 month, and signs of conjunctival, corneal and systemic inflammation were periodically checked. To ascertain the effectiveness of the surgery, tear volume was measured using a phenol red thread (Zone-Quick, Menicon, Nagoya, Japan) before the surgery (at 2 months of age) and on the day of electrophysiological recording 4 weeks later (at 3 months of age).

2.4 | Light stimulation

To induce photoisomerization of DENAQ, an LED emitting at a wavelength of 460 nm (Prizmatix Ltd., Holon, Israel) was used (Figure 1a,c). The incident light intensity at the cornea was 60 mW·cm^{-2}. The light protocol consisted of five cycles of alternating dark/light pulses (photocycles) of 15 s each, followed by three consecutive cooling ramps from 34°C to 15°C of 30-s duration at an average cooling rate of −0.5°C·s^{-1}. The first and third cooling ramps were conducted under dark conditions, whereas the second was performed under light irradiation (Figure 3a). The light-induced change in the NTI frequency of cold nerve terminals that were pre-incubated with DENAQ was referred to as photoswitching (PS) and was calculated as follows:

$$\frac{\text{NTI frequency in dark} - \text{NTI frequency in light}}{\text{NTI frequency in dark}} \times 100$$

For all electrophysiological recordings in guinea pigs, it was considered that a change in the same direction should occur five times because five photocycles were applied to each nerve terminal to evaluate photoswitching.

2.5 | Immunohistochemistry

The immuno-related procedures used comply with the recommendations made by the *British Journal of Pharmacology* (Alexander et al., 2018). TRPM8^{BAC}–EYFP mice were humanely killed with an intraperitoneal overdose of sodium pentobarbital (Dolethal, Vetoquinol, Lure, France), followed by cervical dislocation. The eyes were then carefully enucleated and fixed in methanol and DMSO (4:1) for 2 h at room temperature (22°C). Afterward, the eyes were incubated for 5 min at −20°C in 100% methanol, rehydrated and washed five times in phosphate-buffered saline (PBS) (5 × 15 min). The corneas were isolated, cut into quadrants and incubated for 2 h at room temperature in a blocking solution containing 5% normal goat serum (Vector Laboratories, Burlingame, CA, USA), 1% bovine serum albumin (Vector Laboratories) and 0.1% Triton X-100 (Sigma-Aldrich) at room temperature for 2 h. Subsequently, the corneas were incubated with primary antibodies diluted in the blocking solution for 4 days at 4°C. Rabbit anti-P2X2 (1:50; Alomone Labs Cat# APR-016, RRID:AB_2313760) and anti-P2X3 (1:50; Alomone Labs Cat# APR-003, RRID:AB_2040054), mouse anti-neuronal class III β-tubulin (1:500; Covance Cat# MMS-435P, RRID:AB_2313773) and chicken anti-GFP (1:500; Abcam Cat# ab13970, RRID:AB_300798) were utilized. After rinsing with PBS, corneas were incubated with secondary antibodies Alexa Fluor 488 goat anti-chicken IgG (1:500; Molecular Probes Cat# A-11039, RRID:AB_142924), Alexa Fluor 555 goat anti-mouse IgG (1:500; Thermo Fisher Scientific Cat# A32727, RRID:AB_2633276) and Alexa Fluor 647 goat anti-rabbit IgG (1:500; Thermo Fisher Scientific Cat# A32733, RRID:AB_2633282) in PBS for 2 h at room temperature, followed by incubation with Hoechst 33342 at 10 µg·ml^{-1} (Thermo Fisher Scientific, Waltham, MA, USA) for 10 min at room temperature. After rinsing with PBS, corneas were mounted with Fluoromount-G (Thermo Fisher Scientific).

Fluorescence images were captured with a Zeiss LSM 880 laser scanning confocal microscope equipped with an LD LCI Plan-Apochromat 25×/0.8 Imm Korr DIC M27 objective (Carl Zeiss AG). The images were analysed using Fiji software (ImageJ 1.4, NIH).

2.6 | Orbicularis oculi electromyography (OOemg) recording

Under isoflurane anaesthesia, Wistar rats (two female/one male) were placed in a stereotaxic frame, and vital constants were monitored and maintained within physiological values. A pair of Teflon-coated steel wires (0.002-in. bare diameter, 0.0045-in. coated diameter; A-M Systems, WA, USA) with 1 mm exposed at the tip was implanted near the temporal and frontal portions of the orbicularis oculi muscle for chronic recording of OOemg signals. The recording wires were led to a connector that was firmly adhered to the skull using acrylic dental resin (DuraLay®, Reliance, IL, USA) and four stainless steel screws. A silver wire (0.005-in. bare diameter, 0.007-in. coated diameter; A-M Systems) connected to one of the screws served as ground. The animals received analgesic treatment (0.05-mg·kg^{-1} buprenorphine, Buprecare® 0.3 mg·ml^{-1}, DFV, Spain) for 3 days following surgery and were kept isolated to prevent any implant damage. Rats were allowed to recover for 10 days before the recording session. Then, the rats were anaesthetised again, and the electrical OOemg signals evoked by cold and heat stimuli were recorded. OOemg activity was amplified, band-pass filtered (300–3000 Hz), digitized and stored using an interface (Micro3 1401, CED, Cambridge, UK) and specific software (Spike2 v7.0, CED, Cambridge, UK) for offline analysis. The number of blinks elicited by each stimulus, as well as the duration, and the area under the curve (AUC) of the evoked response were analysed.

The ocular surface thermal stimulation was performed by instilling on the cornea 20-µl saline drops at different temperatures. Cold stimuli induced a decrease in ocular surface temperature from the basal temperature (32°C to 30°C) down to 15°C. Saline drops producing temperature increases up to 40°C to 42°C were used for noxious heat stimulation. The temperature of the ocular surface was continuously recorded with a high-speed thermal probe (IT-24P, Physitemp, BAT-12, Clifton, NJ, USA) placed in close contact with the cornea. Stimuli were spaced at least 30 s apart to allow the ocular surface temperature to return to its basal value after each stimulus. The dark/light conditions were alternated under basal conditions. Then animals were treated topically with DENAQ. For this purpose, 10-µl drops of 20-mM DENAQ were instilled onto the ocular surface at regular intervals of 30 s, for 40 min.

2.7 | Data and statistical analysis

The data and statistical analysis comply with the recommendations of the *British Journal of Pharmacology* on experimental design and analysis in pharmacology (Curtis et al., 2025). Data were collected and processed for statistical analysis using a free trial of GraphPad Prism 9 software (GraphPad, San Diego, CA, USA). The Shapiro–Wilk normality test was initially applied to data samples. Non-normally distributed data are presented as median and interquartile range (IQR = 25% quartile to 75% quartile), while normally distributed data are expressed as mean ± SEM. A P value of 0.05 or less was considered significant. When comparing two samples, either a t test or a non-parametric equivalent was applied. For comparing multiple samples, either ANOVA or a non-parametric counterpart was used. The specific tests are indicated in the text and figure captions.

2.8 | Materials

DENAQ was synthesized according to Mourot et al. (2011) and obtained from Jubilant Chemsys, Ltd. (Noida, UP, India). It was dissolved in dimethyl sulfoxide (DMSO; Sigma-Aldrich, St. Louis, MO, USA) at a stock concentration of 200 mM. Stock solutions were prepared by dissolving the drug in distilled water at the following concentrations: cilobradine (24.01 mM; Sigma-Aldrich), capsazepine (100 mM; Tocris Bioscience, Bristol, UK), suramin hexasodium salt (50 mM; Tocris Bioscience), TNP-ATP triethylammonium salt (10 mM; Tocris Bioscience) and purotoxin-1 (0.1 mM; Smartox Biotechnology, Saint-Égrève, France). A stock solution of A740003 from Sigma-Aldrich dissolved in ethanol at a concentration of 20 mM was also prepared. All chemicals were then diluted to their respective working concentrations with the physiological solution.

2.9 | Nomenclature of targets and ligands

Key protein targets and ligands in this article are hyperlinked to corresponding entries in http://www.guidetopharmacology.org and are permanently archived in the Concise Guide to PHARMACOLOGY 2023/24 (Alexander, Fabbro, Kelly, Mathie, Peters, Veale, Armstrong, Faccenda, Harding, Davies, Amarosi, et al., 2023; Alexander, Fabbro, Kelly, Mathie, Peters, Veale, Armstrong, Faccenda, Harding, Davies, Annett, et al., 2023; Alexander, Mathie, Peters, Veale, Striessnig, Kelly, Armstrong, Faccenda, Harding, Davies, Aldrich, et al., 2023).

3 | RESULTS

3.1 | DENAQ confers light sensitivity to the spontaneous activity of corneal cold nerve terminals

Nerve terminal impulse (NTI) activity was measured in cold nerve terminals of excised guinea pig corneas pre-incubated with DENAQ. Cold thermoreceptor terminals fired spontaneous NTIs at 34°C. The frequency markedly increased in response to a cooling ramp down to 15°C, allowing their identification and characterization (Figure 2a,b).

Before being exposed to light, cold nerve terminals that were treated with 200-μM DENAQ showed a lower frequency of spontaneous NTI, compared to untreated terminals (Figure 2c,d).

DENAQ is a red-shifted optochemical that undergoes a rapid *trans*-to-*cis* conversion upon exposure to light in the visible spectrum, with a peak at 470 nm (Mourot et al., 2011). It returns to its *trans* form in the dark (Figure 1b). To determine the effect of DENAQ photoisomerization on the electrical activity of peripheral sensory nerve terminals isolated from their cell bodies, an LED was used to deliver light at 460 nm in five photocycles, as shown in Figure 2a,b. We first observed that light exposure did not affect spontaneous activity in untreated corneas (Figure 2c). In contrast, the mean spontaneous activity of cold thermoreceptors pre-incubated with DENAQ was significantly lower upon light irradiation compared to the activity displayed in the dark in 9 out of 15 cold nerve terminals (Figure 2d). Notably, spontaneous activity increased in the dark after each light pulse along the five photocycles in corneas pre-incubated with DENAQ (Figure 2b,d).

Together, these results demonstrate that DENAQ, in addition to pharmacologically blocking the spontaneous activity of cold nerve terminals, allows its photoreduction on the guinea pig cornea.

3.2 | DENAQ does not affect cold-evoked responses of corneal sensory nerve terminals

We next investigated whether DENAQ could photomodulate responses to cold at the nerve terminal. Cooling ramps were applied to corneas pre-treated with 200-μM DENAQ in the dark or during LED irradiation (Figure 3a). The first cooling in the dark ramp evoked a median peak frequency of NTIs at cold thermoreceptors which was not significantly different from the frequency under LED irradiation (Figure 3b). Furthermore, the cooling threshold in the dark did not significantly differ from that in the light (Figure 3c). These results show that DENAQ does not photomodulate the cold-evoked nerve activity on the guinea pig cornea.

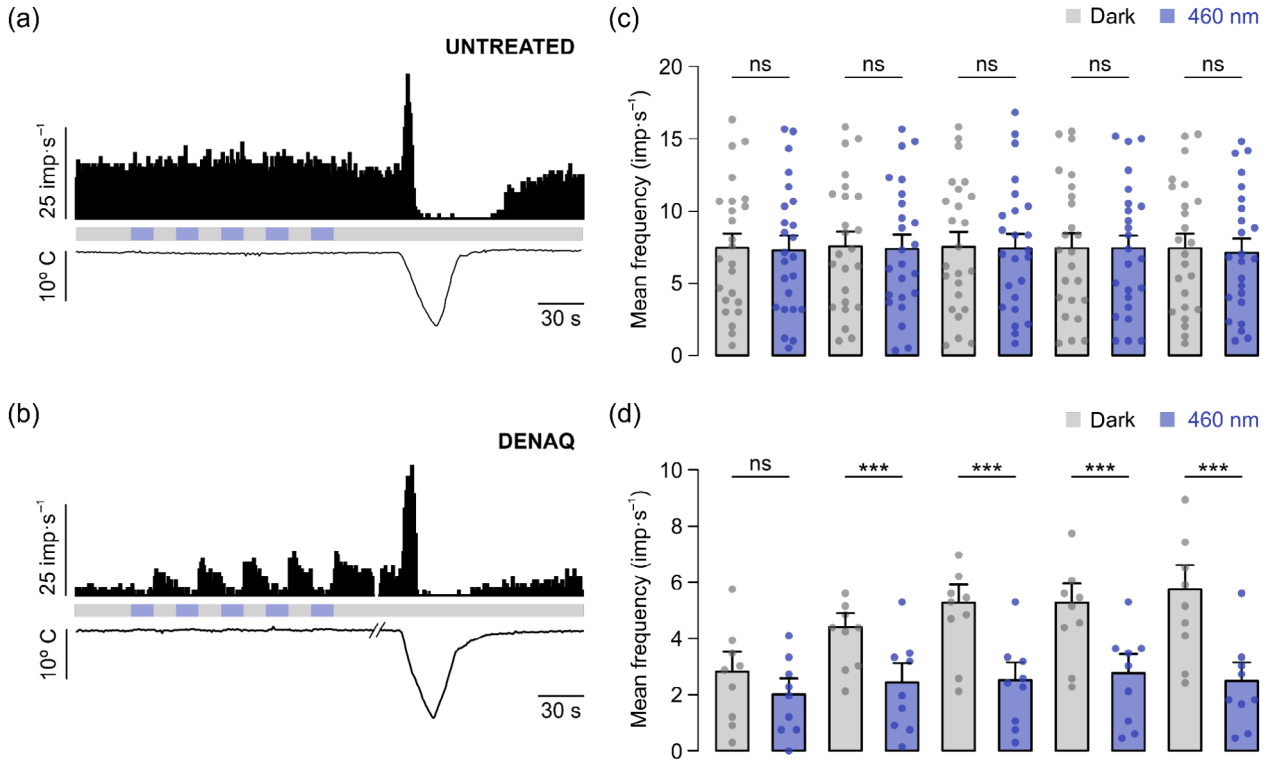

FIGURE 2 Photomodulation of the spontaneous activity of cold nerve terminals in excised guinea pig corneas pre-incubated with DENAQ. Spontaneous activity rate histogram during a recording period that includes five photocycles of darkness/460-nm LED illumination in an untreated cornea (a) and a cornea pre-incubated with 200-μM DENAQ (b). Mean frequency recorded during light application (in blue) and dark (in grey) from non-incubated (n = 24 nerve terminals, 12 animals) (c) and DENAQ pre-incubated corneal cold nerve terminals (n = 9 nerve terminals, 3 animals) (d). Note that the mean NTI frequency was lower (P<0.001; Student t-test) in DENAQ pre-incubated (first bar in grey) in comparison to non-incubated corneas (first bar in grey). The percentage of spontaneous NTI frequency reduction in response to light irradiation compared to dark conditions was statistically significant in DENAQ-preincubated corneal cold nerve terminals (PS = 46.0 ± 2.3%, n = 45 photocycles, P < 0.001, one-sample t-test) (c), in contrast to untreated DENAQ nerve terminals (PS = −1.3 ± 2.3%, n = 120 photocycles, one-sample t-test) (d). Differences in NTI mean frequency between light and dark conditions within each photocycle were compared using one-way repeated measures ANOVA. ***P ≤ 0.001, significantly different as indicated, ns, not significant; Holm–Šidák method.

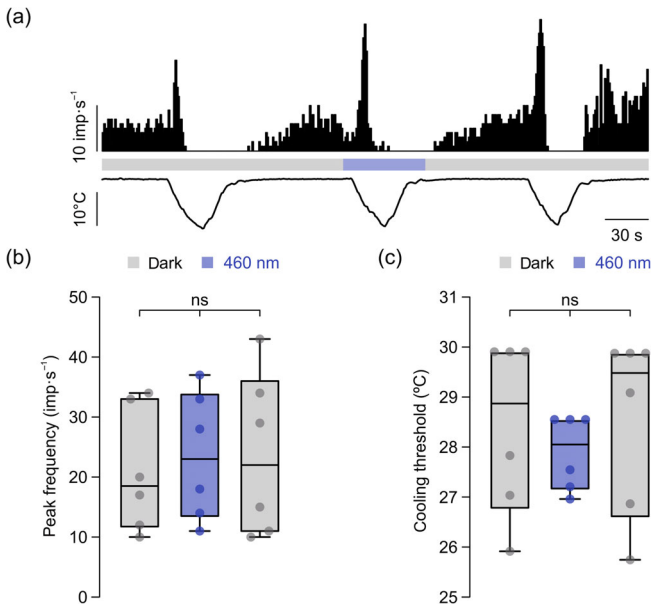

FIGURE 3 Effects of light on cold-evoked responses of nerve terminals in excised corneas pre-incubated with DENAQ. (a) Sample rate histogram of the nerve terminal impulses (NTIs) at corneal nerve terminals pre-incubated with DENAQ (200 μM) in response to cooling ramps in darkness (grey bar) and upon LED illumination (blue bar). (b) Box plot showing the frequency of NTIs at the peak response reached under cold stimulation and (c) cooling threshold temperature in darkness (grey boxes) and light conditions (blue box). Each dot represents the corresponding value from a single cold nerve terminal. Data shown are medians with interquartile ranges (from first to third quartile) (n = 6 nerve terminals, 3 animals). Friedman one-way repeated measures ANOVA on ranks; all pairwise multiple comparison procedures by Dunn's method. ns, not significant.

3.3 | Mechanistic insights into the interaction of DENAQ and potassium channels at the corneal nerve terminal

The shape of NTIs in corneal cold nerve terminals pre-incubated with 200-μM DENAQ was then analysed (Figure 4). In corneas pre-incubated with DENAQ (three animals), the half-width of the negative component of the NTI was significantly shorter under LED light irradiation than in darkness (Figure 4a,b). Consistent with the previously described *trans* blocker effect of DENAQ on K_V channels (Tochitsky et al., 2014, 2016), these results suggest that DENAQ blocks K_V channels in the *trans* configuration (dark) and partly releases inhibition in the *cis* configuration (light).

In addition to K_V channels, DENAQ also blocked HCN channels in the *trans* configuration (Ko et al., 2016; Tochitsky et al., 2014, 2016). To explore the potential role of HCN channels in the photoswitching of the cold terminal spontaneous activity, corneas were pre-incubated with 2-mM DENAQ (two animals) and subjected to five photocycles of light at 460 nm. Then, the HCN channel blocker **cilobradine** (Stieber et al., 2006) was perfused at a concentration of 100 μM for 1 min before and during the light protocol application. In three cold terminals pre-incubated with DENAQ, the photoswitching effect was not significantly changed by cilobradine (37.0 ± 3.6%, n = 15 photocycles before; and 42.0 ± 6.5%, n = 15 photocycles during cilobradine perfusion). These results suggest that K_V channels, but not HCN channels, are primarily responsible for the DENAQ-mediated photoswitching effect on the ongoing activity of corneal cold sensory nerve terminals.

3.4 | P2X channel blockers prevent DENAQ-mediated photomodulation in corneal cold nerve terminals

P2X2 and **P2X3** channels have previously been identified in the soma of trigeminal neurons (Staikopoulos et al., 2007). However, it remains unclear whether they are present and functional at their nerve terminals (Dowd et al., 1997; Matthews et al., 1997). Interestingly, the membrane-impermeant compound DENAQ can be used as an ultrasensitive reporter of the functional expression of P2X receptors in retinal ganglion cells due to its ability to permeate these large-pore channels (Tochitsky et al., 2016). Here, the potential role of **ATP-gated purinergic receptors** and transient receptor potential **(TRP)** channels in the entry of DENAQ into the cold nerve ending was investigated. Excised corneas were pre-incubated with 2-mM DENAQ plus a pharmacological antagonist of the P2X receptor or transient receptor potential vanilloid 1 (**TRPV1**) and TRPM8 channels. As shown in Figure 5, cold nerve terminals co-incubated with DENAQ and **suramin**, a non-selective antagonist of **purinergic P2 receptors** (Dunn & Blakeley, 1988; Hoyle et al., 1990), or DENAQ with the P2X receptor inhibitor **TNP-ATP** (Virginio et al., 1998), or DENAQ with the selective **P2X3 receptor** blocker purotoxin-1 (Grishin et al., 2010; Kabanova et al., 2012) showed a significantly smaller DENAQ-mediated photoswitching than those cold nerve terminals pre-incubated with DENAQ alone. However, no statistical differences were observed when comparing the photoswitching in cold nerve terminals pre-incubated with DENAQ alone and those pre-incubated with DENAQ together with A740003, a selective antagonist of the **P2X7** receptor (Honore et al., 2006) or the TRPV1 and TRPM8 antagonist **capsazepine** (Behrendt et al., 2004; Bevan et al., 1992). In the latter case, a reduced photoswitching was observed in 7 out of 12 terminals, so a TRPV1- or TRPM8-mediated permeation of DENAQ into the cold-sensing nerve endings cannot be ruled out.

An immunoreactivity assay identified the immunohistochemical expression of P2X2 and P2X3 receptors in mouse corneal cold terminals. To achieve this, we utilized a genetically modified mouse that expresses EYFP under the promoter of the cold-sensing ion channel TRPM8. Additionally, sub-basal nerve fibres (Figure 6a–d) and nerve terminals (Figure 6e–h) located at the corneal epithelium were immunolabelled with anti-β-III-tubulin, anti-GFP, anti-P2X2 and anti-P2X3. As shown in Figure 6, staining for P2X2/P2X3 receptors was present in both the corneal cold sensory nerve fibres and their nerve terminals.

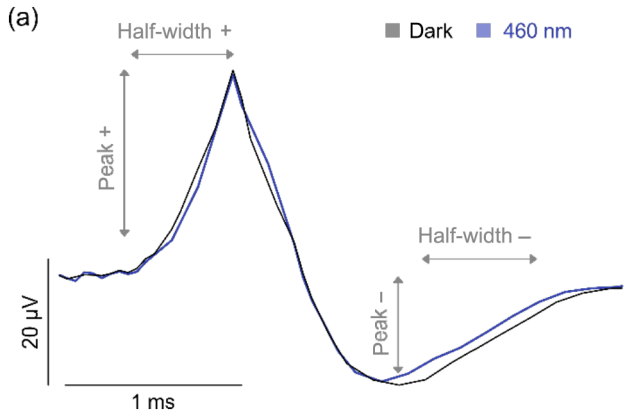

(b)

	Dark	460 nm
Peak + (mV)	0.032 ± 0.007	0.031 ± 0.006
Peak – (mV)	–0.018 ± 0.005	–0.018 ± 0.005
Half-width + (ms)	0.552 ± 0.057	0.552 ± 0.061
Half-width – (ms)	1.170 ± 0.132	1.108 ± 0.127**

FIGURE 4 Effects of light on the nerve terminal impulse (NTI) shape in corneas pre-treated with DENAQ. (a) NTI waveform under darkness and 460-nm light. The average shape of 200 NTIs recorded under each condition in nine cold sensory nerve terminals is shown. (b) Table summarizing mean ± SEM of the different parameters analysed to quantify the NTI shape. *P < 0.05, significant difference between dark and light conditions; paired t test.

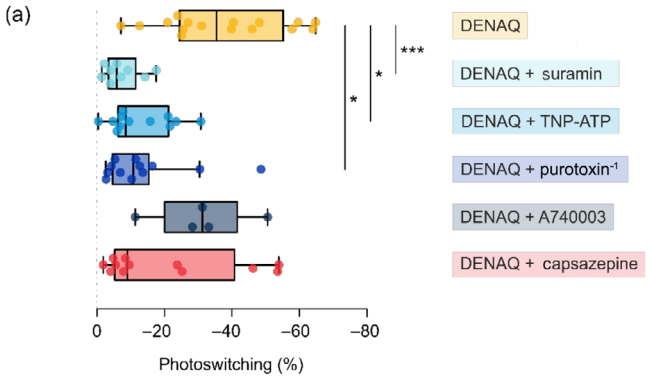

FIGURE 5 Photoswitching effect of DENAQ on the spontaneous activity of guinea pig corneal cold thermoreceptor nerve terminals in the presence of P2X receptor antagonists and TRPV1 channel antagonists. Data shown are the photoswitching value calculated for each cold nerve terminal shown as individual values with medians and interquartile ranges (from first to third quartile). Samples sizes as follows: DENAQ, n = 16 terminals, 7 animals; DENAQ + suramin, n = 9 terminals, 3 animals; DENAQ + TNP-ATP, n = 12 terminals, 3 animals; DENAQ + purotoxin 1, n = 12 terminals, 6 animals; DENAQ + A740003, n = 5 terminals, 5 animals; DENAQ + capsazepine, n = 12 terminals, 5 animals. *P < 0.05, ***P < 0.001, significantly different as indicated; Kruskal–Wallis ANOVA on ranks; all pairwise multiple comparison procedures by Dunn's method.

These results indicate that DENAQ primarily enters corneal cold sensory nerve endings through P2X channels, suggesting the functional expression of P2X3 channels at corneal cold sensory terminals.

3.5 | DENAQ photoreduces the spontaneous activity of cold nerve endings in tear-deficient corneas

Excised guinea pig corneas with surgically induced eye surface dry condition were pre-treated with 200-µM DENAQ. Consistent with earlier research (Kovács et al., 2016), the spontaneous activity of tear-deficient cold nerve terminals showed a higher NTI frequency, compared with that of naïve corneas (Figure 7b).As observed with the naïve cold nerve terminals, blue light irradiation reduced the spontaneous activity in cold nerve terminals of tear-deficient animals, compared to dark conditions (Figure 7a,b).

However, LED irradiation did not affect the cold-evoked response in DENAQ-pre-treated nerve terminals of tear-deficient guinea pigs. The median of the peak frequency of NTIs cold thermoreceptors evoked by the first cooling ramp in the dark was not significantly different from that during LED irradiation (Figure 7c). Furthermore, the cooling threshold, in the dark was not significantly different from that in the light (Figure 7d).

These results indicate that DENAQ allows the photoreduction of the pathologically enhanced spontaneous cold nerve terminal activity in a guinea pig model of tear-deficient DE without affecting the response to cold.

3.6 | DENAQ photosensitizes cold-induced electromyography activity of the orbicularis oculi muscle

Corneal sensory receptors have been reported to modulate blink rate in rodents and humans (see Acosta et al., 1999; Quallo et al., 2015). Therefore, we asked whether DENAQ could mediate in vivo photomodulation of thermally-induced blink reflexes. To this end, 20-mM DENAQ was applied to the ocular surface of three anaesthetized adult rats, and the cold-evoked OOemg activity was measured in the dark and under blue light illumination (Figure 8a). Prior to the treatment with DENAQ, the number of cold-evoked blinks under light irradiation was lower, the AUC of the cold-evoked OOemg signal was diminished and its duration was reduced upon illumination, relative to dark conditions (Figure 8b–d). After DENAQ application, the number of cold-evoked blinks was higher under blue light, the AUC was greater and the OOemg activity duration was longer upon

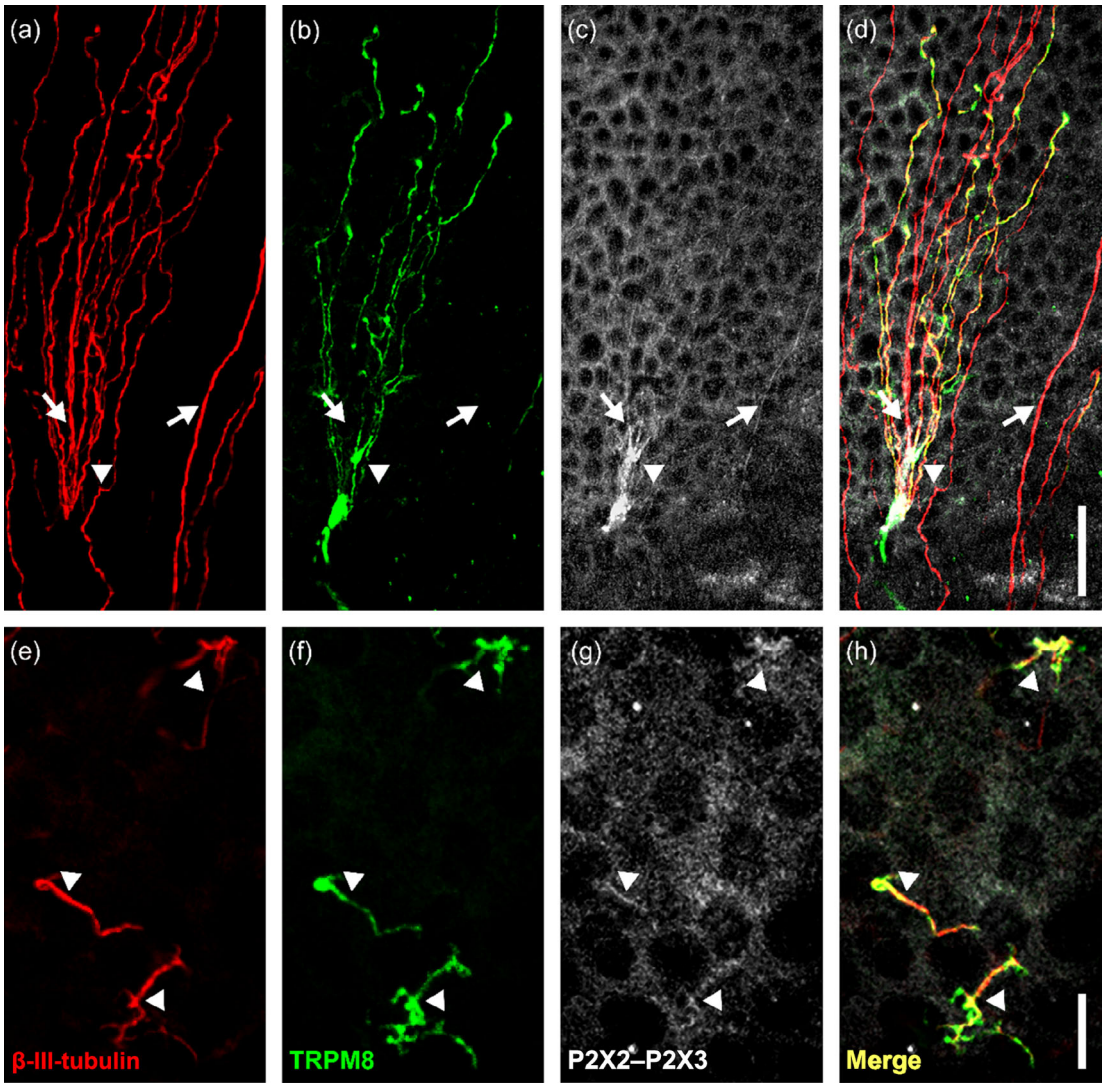

FIGURE 6 Immunohistochemical identification of P2X2 and P2X3 receptors in TRPM8-expressing corneal nerve terminals. Maximal projection of z-stacked confocal images of corneal cold nerves in a whole-mounted cornea from a $TRPM8^{BAC}$–EYFP mouse is shown. Sub-basal nerve fibres (a–d) and their intraepithelial nerve endings (e–h) were immunolabelled with anti-β-III-tubulin (red), anti-GFP (green), and anti-P2X2 and anti-P2X3 (grey). Arrowheads indicate positive sub-basal nerve fibres and positive nerve endings for TRPM8, P2X2 and P2X3. Arrows indicate positive sub-basal nerve fibres only for P2X2 and P2X3. Scale bars: (a–d) 30 μm; (e–h) 15 μm.

illumination, compared to values under dark conditions (Figure 8a–d). Notably, no significant differences in the heat-evoked blink reflex were observed when comparing blue light and dark conditions (Figure 8e–h).

The results indicate the presence of in vivo DENAQ photomodulation of the cold-evoked but not the heat-evoked blink reflex in anaesthetized rats, thereby supporting the involvement of corneal sensory receptors, particularly those sensitive to moderate and intense cold, such as cold thermoreceptors and polymodal nociceptors.

4 | DISCUSSION

We have demonstrated that the photoisomerizable small-molecule DENAQ confers light sensitivity to guinea pig cold sensory nerve endings on excised corneas. Previous research has shown that DENAQ photosensitizes retinal ganglion cell activity in a mouse model of **retinitis pigmentosa**, as well as binaural auditory gerbil neurons (Ko et al., 2016; Tochitsky et al., 2016). Our data further demonstrate that DENAQ modulates the electrical activity of peripheral sensory axons separated from their soma in a light-dependent manner. This adds to the body of evidence that azobenzene-based small molecules can make nociceptors sensitive to light directly at their nerve terminals (Frank et al., 2015; Landra-Willm et al., 2023; Mourot et al., 2012).

DENAQ *is a trans*-blocker of both K_V and HCN channels in the dark, whereas high-intensity visible light converts DENAQ to its *cis*-isomer, thereby releasing them from blocking (Mourot et al., 2011; Tochitsky et al., 2014). Therefore, DENAQ's effect on cold nerve terminal excitability is expected to be a balance of the hyperpolarizing or depolarizing contributions of these ion channels to the nerve terminal

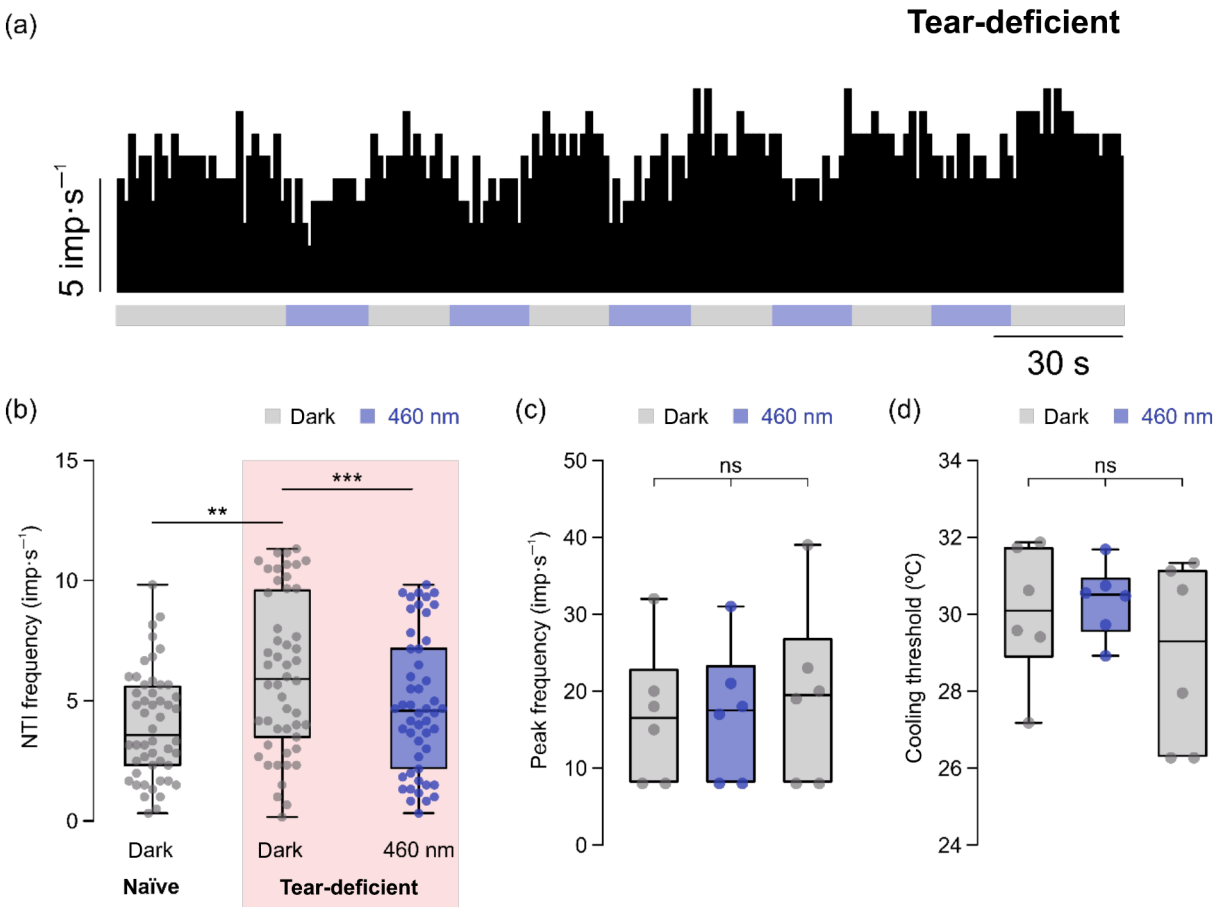

FIGURE 7 Photomodulation of the spontaneous activity of cold nerve endings in tear-deficient and naïve corneas pre-treated with DENAQ. (a) Spontaneous activity rate histogram along the five cycles of darkness/460-nm LED illumination in tear-deficient corneas pre-incubated with DENAQ at 200 μM. (b) Corneal cold nerve terminal spontaneous NTI frequency recorded during blue light application (box plot in blue) and in dark conditions (box plots in grey) in DENAQ-treated naïve and tear-deficient corneas (red shading). Every dot represents the NTI frequency value corresponding to a photocycle under the above-described conditions (**$P < 0.01$ and ***$P < 0.001$). (c) Maximum firing frequency during the response to cold stimulation. (d) Cooling threshold temperature (absolute value). Each dot represents the corresponding value from a cold nerve terminal. The centre line is the median, and the bounds of the box are interquartile ranges (first to third). Friedman one-way repeated measures ANOVA on ranks; all pairwise multiple comparison procedures by Dunn's method. ns, not significant.

membrane potential. In the dark, the ongoing cold nerve terminal activity decreased, suggesting that the hyperpolarizing effect of pharmacological blockade of HCN channels predominated over the depolarizing effect of pharmacological inhibition of K_V channels by DENAQ. In support of the proposal that inhibition of HCN channels by DENAQ in the dark reduced the spontaneous activity, previous data from our laboratory have shown that the HCN channel chemical antagonists **ivabradine** and their structural derivatives cilobradine and zetabradine reduced the spontaneous activity of corneal cold nerve terminals (Quirce, 2020).

Light irradiation decreased ongoing cold nerve terminal activity to a greater extent than pretreatment with DENAQ alone, suggesting a hyperpolarizing effect through the photo-release of K_V channel conductance from blocking, which overcomes the depolarizing effect of photo-release on HCN channel activity. This is supported by the persistence of DENAQ-mediated photoswitching in the presence of the HCN blocker cilobradine. In line with this, several K_V channel subtypes, including **K_V 2.1**, **K_V 3.1** and **K_V 4.2** (Mourot et al., 2013), which are present in rodent primary sensory neurons (Bocksteins et al., 2012), are photomodulated by DENAQ when heterogeneously expressed in HEK293 cells. Additional evidence supporting the contribution of K_V channels to DENAQ-mediated photoswitching in the cold nerve terminal is derived from the NTI shape analysis. Cold nerve terminals recorded extracellularly exhibit a biphasic (positive–negative) shape in NTIs. The configuration of NTI corresponds to the first derivative of the voltage membrane of the nerve terminal. The positive deflection is associated with membrane depolarization, while the negative deflection is associated with membrane repolarization mediated by K_V channel openings (Brock et al., 2001, 2006). We found that spontaneous NTIs generated at cold sensory nerve terminals in corneas pre-incubated with DENAQ exhibited a more prolonged negative phase of 53% of its half-width in the dark (*trans* isomer), rapidly shortened by LED irradiation (*cis* isomer) up to 41%. This suggests that light exposure partly unblocks the 22.6% of the Kv

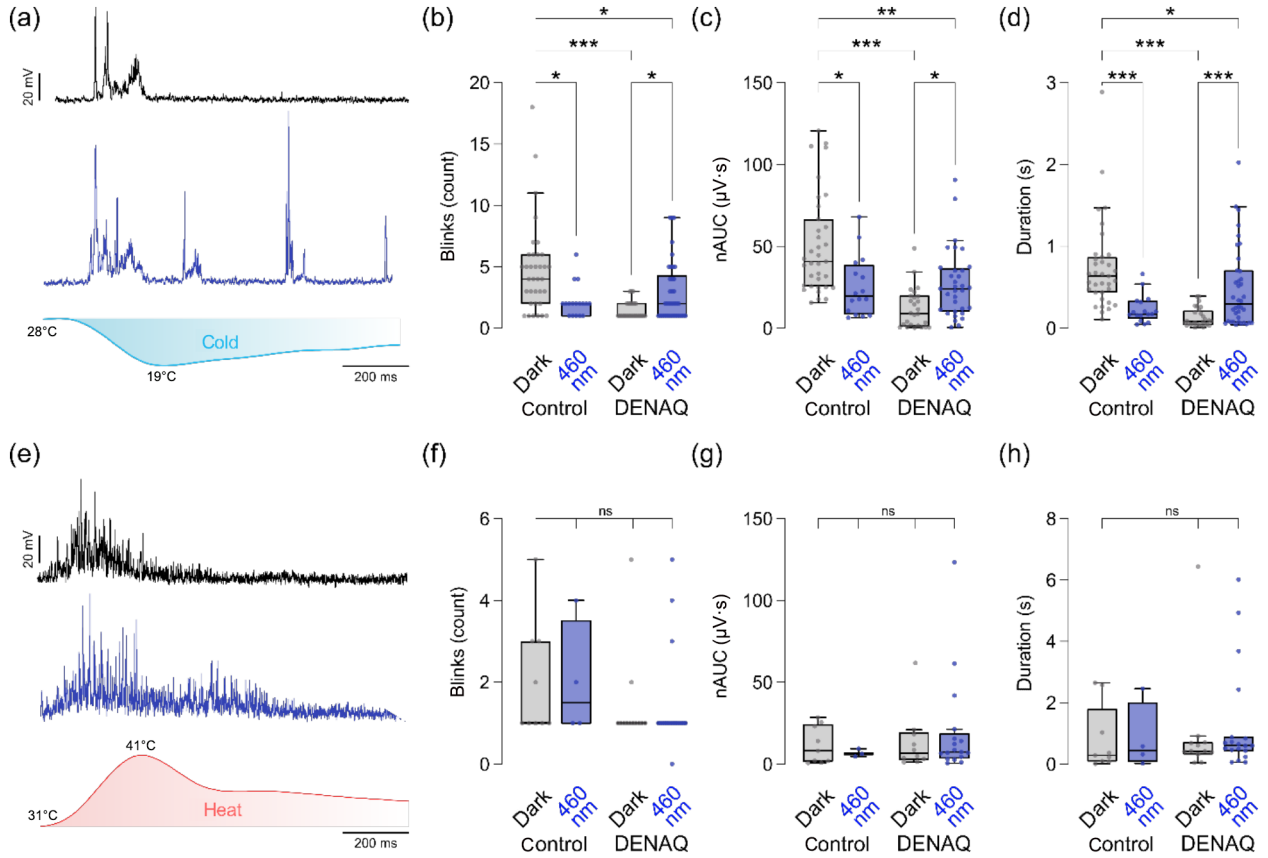

FIGURE 8 Photomodulation of the thermal reflex blink with DENAQ. Typical recordings of evoked OOemg activity in response to ocular surface cooling up to 18°C (blue) (a) and heating up to 41°C (red) (e) after topical administration of DENAQ to the eyes of anaesthetised rats. OOemg recordings under 460-nm LED irradiation are highlighted in blue and grey under dark conditions. The number of blinks induced by cooling is shown in (b) or heating in (f). The net area under the curve (nAUC) of the OOemg signal in response to cold is shown in (c) and heat in (g). The duration of the OOemg signal evoked by ocular surface cooling is presented in (d) and heat in (h). The box plots in blue correspond to blue light application, and the box plots in grey correspond to dark conditions. Data shown are individual values with medians and interquartile ranges (from first to third quartile). $^{*}P < 0.05$, $^{**}P < 0.01$, $^{***}P < 0.001$; significantly different as indicated; ns, not significant; Kruskal–Wallis ANOVA on ranks, followed by all pairwise multiple comparison procedures using Dunn's method.

channel activity blocked by DENAQ in the dark, which is consistent with the partial photoreduction of spontaneous activity of cold nerve terminals pre-incubated with DENAQ. In support of this, the photoswitching of the activity of recombinant $K_V3.1$ channels expressed in HEK293 cells has been revealed to be partial (Mourot et al., 2011). This suggests that native K_V channels at the corneal nerve terminals may also undergo partial photoswitching. However, a comprehensive investigation would be necessary to elucidate whether this partial release of K_V activity is entirely responsible for the photoswitching of the cold nerve terminal. The DENAQ molecule terminates in a quaternary ammonium ion on one side of the azobenzene, which interacts with the **tetraethylammonium (TEA)** binding site in the inner lumen of the channel (Mourot et al., 2011). Consistent with our findings, TEA prolongs the duration of the NTI-negative phase in guinea pig corneal cold receptors (Brock et al., 2006). Additionally, TEA does not affect the response of guinea pig corneal cold receptors to cooling (Brock et al., 2006). Similarly, our study demonstrates that DENAQ does not photomodulate cold-evoked responses in corneal nerve endings.

Of note, we observed that the ongoing cold nerve terminal activity in the dark after each light application increased compared to the value before the light application. This may indicate insufficient time for DENAQ to re-block the HCN channels before the following light irradiation pulse. It is worth noting that DENAQ converts from the *trans* to *cis* state rapidly within milliseconds upon light exposure, but it takes seconds for DENAQ to thermally convert back to its default *trans* state (Mourot et al., 2011).

P2X channels have been implicated in central and peripheral pain mechanisms (Burnstock, 2000; Inoue, 2022). P2X3 mRNA and protein have been found primarily in small-diameter non-peptidergic cell bodies of primary sensory neurons (Chen et al., 1995; Eriksson et al., 1998; Lewis et al., 1995). The channels either form homo-oligomeric channels or assemble with P2X2 subunits to form hetero-oligomers (North, 2004). Additionally, a fraction of peripheral projections of sensory neurons in the skin, tongue and dental pulp are immunopositive for P2X3 in rodents (Bo et al., 1999; Burnstock, 2000). This study investigated the expression of P2X2 and P2X3 subunits in TRPM8–EYFP-positive corneal nerve terminals in

adult mice. We observed P2X and P2X3 receptor staining at identified cold sensory nerve terminals. Consistent with the immunochemical expression of the nociceptive markers P2X3 receptor and CGRP protein in small subsets of mouse dorsal root ganglion cell bodies expressing TRPM8 (Takashima et al., 2010), our results indicate that a fraction of TRPM8 nerve terminals also express P2X2 and P2X3 receptors.

The functionality of P2X channels at corneal sensory nerve terminals remains uncertain. While purinergic P2X receptor agonists have been shown to excite rat joint nociceptors (Dowd et al., 1998), attempts to stimulate cat dental pulp afferents (Dowd et al., 1997) or cat corneal nociceptors (Matthews et al., 1997) have been unsuccessful. In addition to species differences, these discrepancies may be explained by specific pharmacological limitations associated with the different experimental models (Dowd et al., 1998). The compound DENAQ is permanently charged, making it relatively impermeable through the cell membrane. A previous study has shown that DENAQ enters neurons through the large-pore P2X channels in retinal ganglion cells from a mouse model of retinitis pigmentosa (Tochitsky et al., 2016). In this work, we demonstrate that the use of purotoxin-1 to selectively block P2X3 receptors partly prevents DENAQ-mediated photoswitching. Notably, primary sensory neurons express the P2X3 receptor protein at a higher level than the other **P2X1–6** receptor subunits, while the P2X7 receptor protein has not yet been identified (Dunn et al., 2001; Flegel et al., 2015; Staikopoulos et al., 2007). Our data suggest that, in guinea pigs, DENAQ enters cold sensory nerve terminals in the cornea, through P2X channels, primarily P2X3 channels. This indicates functional expression of P2X channels at the nerve terminal.

In patients with dry eye disease, ectopic activity at corneal cold nerve endings can cause discomfort, pain, altered blinking and a sensation of dryness (Belmonte et al., 2017). Here, we show that DENAQ reduces spontaneous activity in corneal cold nerve endings in guinea pig tear-deficient corneas in response to light but not cold-evoked responses. This finding suggests that DENAQ may be a beneficial treatment in patients with dry eye, as it can alleviate ocular discomfort or pain without compromising the cold sensation and cold-evoked reflexes essential for maintaining ocular surface integrity. Furthermore, azobenzene-based photoswitches offer a new therapeutic approach that takes advantage of the large-pore characteristic of P2X receptors. This allows for delivering membrane-impermeable drugs specifically to cells with increased P2X receptor expression (Tochitsky et al., 2016). A recent study by Fakih et al. (2021) demonstrated the overexpression of P2X3 receptor mRNA in TG neurons from a mouse model of dry eye. This finding indicates that DENAQ-mediated photomodulation may selectively target altered cold nerve endings over healthy tissue.

In this study, we further provide evidence of the in vivo effect of DENAQ when administered topically in the eye of anaesthetised rats. DENAQ enhanced cold-evoked OOemg activity under blue light, although it did not significantly affect the cold-evoked activity in cold thermoreceptors of guinea pig excised corneas. The observed discrepancy may be attributed to the different animal model used, the higher concentration of DENAQ adapted to in vivo conditions and its delivery beyond the cornea (including the conjunctiva and eyelid border) in the blink reflex paradigm. However, recent work has indicated that corneal polymodal nociceptors may contribute to the mediation of the cold-evoked blink reflex in mice (Frutos-Rincón et al., 2023). Consequently, it is possible that distinct functional classes of corneal sensory nerve terminals, which are not classified as cold thermoreceptors, may be subject to photomodulation by DENAQ in the cold-evoked blink reflex. Further studies are required to elucidate this observation.

In conclusion, the photoisomerizable compound DENAQ confers light sensitivity to the spontaneous activity, but not the cold-evoked responses, of guinea pig corneal cold thermo- receptors. DENAQ primarily enters the corneal cold nerve terminal through P2X channels, whereas K_V channels appear responsible for the DENAQ-mediated photoswitching of its spontaneous activity. DENAQ photoreduces the pathologically enhanced spontaneous cold nerve terminal activity in a guinea pig model of dry eye without affecting the response to cold. Furthermore, DENAQ photomodulated the cold-evoked blink reflex in vivo after topical eye application in rats. Our results support the use of small azobenzene photoswitches as a potential therapeutic strategy for managing ectopic corneal nerve activity. This approach might offer a potential treatment for ocular discomfort and pain in dry eye disease.

AUTHOR CONTRIBUTIONS

David Ares-Suárez: Formal analysis (lead); investigation (lead); methodology (supporting); visualization (lead); writing—original draft (supporting); writing—review and editing (supporting). **Almudena Iñigo-Portugués:** Formal analysis (supporting); investigation (supporting); methodology (supporting); visualization (supporting); writing—original draft (supporting); writing—review and editing (supporting). **Enrique Velasco:** Formal analysis (supporting); investigation (supporting); visualization (supporting); writing—original draft (supporting); writing—review and editing (supporting). **Susana Quirce:** Formal analysis (supporting); investigation (supporting); methodology (supporting); writing—review and editing (supporting). **Fernando Aleixandre-Carrera:** Formal analysis (supporting); investigation (supporting); visualization (supporting); writing—original draft (supporting); writing—review and editing (supporting). **Ariadna Díaz-Tahoces:** Formal analysis (supporting); investigation (supporting); visualization (supporting); writing—original draft (supporting); writing—review and editing (supporting). **M. Carmen Acosta:** Resources (supporting); validation (supporting); writing—review and editing (supporting). **Wan-Chen Lin:** Investigation (supporting); resources (supporting); writing—review and editing (supporting). **Richard H. Kramer:** Conceptualization (supporting); resources (supporting); writing—review and editing (supporting). **Carlos Belmonte:** Conceptualization (supporting); writing—review and editing (supporting). **Juana Gallar:** Conceptualization (supporting); funding acquisition (lead); resources (supporting); supervision (supporting); validation (supporting); writing—original draft (supporting); writing—review and editing (supporting). **Victor Meseguer:** Conceptualization

(lead); data curation (lead); formal analysis (supporting); funding acquisition (lead); investigation (supporting); methodology (supporting); project administration (lead); resources (supporting); supervision (lead); validation (lead); visualization (lead); writing—original draft (lead); writing—review and editing (lead).

ACKNOWLEDGEMENTS

This research was supported by Grants RTI2018-100994-AI00, PID2021-124460OB-I00 (V.M.) and PID2023-147915OB-I00 (J.G. and M.C.A.) funded by MICIU/AEI/10.13039/501100011033 and by ''ERDF A way of making Europe''. Grant CIPROM/2021/48 from the Conselleria de Cultura, Educación y Ciencia, Generalitat Valenciana, Spain, is also acknowledged.

CONFLICT OF INTEREST STATEMENT

The authors declare no conflicts of interest.

DATA AVAILABILITY STATEMENT

The data that support the findings of this study are available from the corresponding author upon reasonable request. Some data may not be made available because of privacy or ethical restrictions.

DECLARATION OF TRANSPARENCY AND SCIENTIFIC RIGOUR

This Declaration acknowledges that this paper adheres to the principles for transparent reporting and scientific rigour of preclinical research as stated in the *BJP* guidelines for Design and Analysis, Immunoblotting and Immunochemistry, and Animal Experimentation and as recommended by funding agencies, publishers and other organizations engaged with supporting research.

ORCID

David Ares-Suárez https://orcid.org/0000-0002-9222-4268
Almudena Iñigo-Portugués https://orcid.org/0000-0003-4368-5495
Enrique Velasco https://orcid.org/0000-0001-7299-0750
Susana Quirce https://orcid.org/0000-0001-9977-357X
Fernando Aleixandre-Carrera https://orcid.org/0000-0002-4739-5033
Ariadna Díaz-Tahoces https://orcid.org/0000-0003-1163-5987
Wan-Chen Lin https://orcid.org/0000-0001-7842-3036
Richard H. Kramer https://orcid.org/0000-0002-8755-9389
Carlos Belmonte https://orcid.org/0000-0001-6891-5942
Juana Gallar https://orcid.org/0000-0002-3559-3649
Victor Meseguer https://orcid.org/0000-0002-7686-6228

REFERENCES

Acosta, M. C., Gallar, J., & Belmonte, C. (1999). The influence of eye solutions on blinking and ocular comfort at rest and during work at video display terminals. *Experimental Eye Research*, *68*(6), 663–669. https://doi.org/10.1006/exer.1998.0656

Acosta, M. C., Luna, C., Quirce, S., Belmonte, C., & Gallar, J. (2013). Changes in sensory activity of ocular surface sensory nerves during allergic keratoconjunctivitis. *Pain*, *154*(11), 2353–2362. https://doi.org/10.1016/j.pain.2013.07.037

Aleixandre-Carrera, F., Engelmayer, N., Ares-Suárez, D., Acosta, M. D. C., Belmonte, C., Gallar, J., Meseguer, V., & Binshtok, A. M. (2021). Optical assessment of nociceptive TRP channel function at the peripheral nerve terminal. *International Journal of Molecular Sciences*, *22*(2), 481. https://doi.org/10.3390/ijms22020481

Alexander, S. P. H., Fabbro, D., Kelly, E., Mathie, A. A., Peters, J. A., Veale, E. L., Armstrong, J. F., Faccenda, E., Harding, S. D., Davies, J. A., Amarosi, L., Anderson, C. M. H., Beart, P. M., Broer, S., Dawson, P. A., Gyimesi, G., Hagenbuch, B., Hammond, J. R., Hancox, J. C., … Verri, T. (2023). The Concise Guide to PHARMACOLOGY 2023/24: Transporters. *British Journal of Pharmacology*, *180*(Suppl 2), S374–S469. https://doi.org/10.1111/bph.16182

Alexander, S. P. H., Fabbro, D., Kelly, E., Mathie, A. A., Peters, J. A., Veale, E. L., Armstrong, J. F., Faccenda, E., Harding, S. D., Davies, J. A., Annett, S., Boison, D., Burns, K. E., Dessauer, C., Gertsch, J., Helsby, N. A., Izzo, A. A., Ostrom, R., Papapetropoulos, A., … Wong, S. S. (2023). The Concise Guide to PHARMACOLOGY 2023/24: Enzymes. *British Journal of Pharmacology*, *180*(Suppl 2), S289–S373. https://doi.org/10.1111/bph.16181

Alexander, S. P. H., Mathie, A. A., Peters, J. A., Veale, E. L., Striessnig, J., Kelly, E., Armstrong, J. F., Faccenda, E., Harding, S. D., Davies, J. A., Aldrich, R. W., Attali, B., Baggetta, A. M., Becirovic, E., Biel, M., Bill, R. M., Caceres, A. I., Catterall, W. A., Conner, A. C., … Zhu, M. (2023). The Concise Guide to PHARMACOLOGY 2023/24: Ion channels. *British Journal of Pharmacology*, *180*(Suppl 2), S145–S222. https://doi.org/10.1111/bph.16178

Alexander, S. P. H., Roberts, R. E., Broughton, B. R. S., Sobey, C. G., George, C. H., Stanford, S. C., Cirino, G., Docherty, J. R., Giembycz, M. A., Hoyer, D., Insel, P. A., Izzo, A. A., Ji, Y., MacEwan, D. J., Mangum, J., Wonnacott, S., & Ahluwalia, A. (2018). Goals and practicalities of immunoblotting and immunohistochemistry: A guide for submission to the British Journal of Pharmacology. *British Journal of Pharmacology*, *175*, 407–411. https://doi.org/10.1111/bph.14112

Behrendt, H. J., Germann, T., Gillen, C., Hatt, H., & Jostock, R. (2004). Characterization of the mouse cold-menthol receptor TRPM8 and vanilloid receptor type-1 VR1 using a fluorometric imaging plate reader (FLIPR) assay. *British Journal of Pharmacology*, *141*, 737–745. https://doi.org/10.1038/sj.bjp.0705652

Belmonte, C., Nichols, J. J., Cox, S. M., Brock, J. A., Begley, C. G., Bereiter, D. A., Dartt, D. A., Galor, A., Hamrah, P., Ivanusic, J. J., Jacobs, D. S., McNamara, N. A., Rosenblatt, M. I., Stapleton, F., & Wolffsohn, J. S. (2017). TFOS DEWS II pain and sensation report. *The Ocular Surface*, *15*(3), 404–437. https://doi.org/10.1016/j.jtos.2017.05.002

Bevan, S., Hothi, S., Hughes, G., James, I. F., Rang, H. P., Shah, K., Walpole, C. S. J., & Yeats, J. C. (1992). Capsazepine: A competitive antagonist of the sensory neurone excitant capsaicin. *British Journal of Pharmacology*, *107*(2), 544–552. https://doi.org/10.1111/j.1476-5381.1992.tb12781.x

Bo, X., Alavi, A., Xiang, Z., Oglesby, I., Ford, A., & Burnstock, G. (1999). Localization of ATP-gated P2X2 and P2X3 receptor immunoreactive nerves in rat taste buds. *Neuroreport*, *10*(5), 1107–1111. https://doi.org/10.1097/00001756-199904060-00037

Bocksteins, E., Van de Vijver, G., Van Bogaert, P., & Snyders, D. (2012). K_v3 channels contribute to the delayed rectifier current in small cultured mouse dorsal root ganglion neurons. *American Journal of Physiology-Cell Physiology*, *303*(4), 406–415. https://doi.org/10.1152/ajpcell.00343.2011

Brock, J. A., Pianova, S., & Belmonte, C. (2001). Differences between nerve terminal impulses of polymodal nociceptors and cold sensory receptors of the guinea-pig cornea. *The Journal of Physiology*, *533*(Pt 2), 493–501. https://doi.org/10.1111/j.1469-7793.2001.0493a.x

Brock, J., Acosta, M. C., Al Abed, A., Pianova, S., & Belmonte, C. (2006). Barium ions inhibit the dynamic response of guinea-pig corneal cold

receptors to heating but not to cooling. *Journal of Physiology*, *575*(2), 573–581. https://doi.org/10.1113/jphysiol.2006.110130

Brock, J., McLachlan, E., & Belmonte, C. (1998). Tetrodotoxin-resistant impulses in single nociceptor nerve terminals in guinea-pig cornea. *The Journal of Physiology*, *512*, 211–217. https://doi.org/10.1111/j.1469-7793.1998.211bf.x

Burnstock, G. (2000). P2X receptors in sensory neurones. *British Journal of Anaesthesia*, *84*(4), 476–488. https://doi.org/10.1093/oxfordjournals.bja.a013473

Chen, C. C., Akopian, A. N., Sivilottit, L., Colquhoun, D., Burnstock, G., & Wood, J. N. (1995). A P2X purinoceptor expressed by a subset of sensory neurons. *Nature*, *377*(6548), 428–431. https://doi.org/10.1038/377428a0

Curtis, M. J., Alexander, S. P. H., Cortese-Krott, M., Kendall, D. A., Martemyanov, K. A., Mauro, C., Panettieri, R. A. Jr., Papapetropoulos, A., Patel, H. H., Santo, E. E., Schulz, R., Stefanska, B., Stephens, G. J., Teixeira, M. M., Vergnolle, N., Wang, X., & Ferdinandy, P. (2025). Guidance on the planning and reporting of experimental design and analysis. *Br J Pharmacol.*, *182*, 1413–1415. https://doi.org/10.1111/bph.17441

Dowd, E., Gallar, J., McQueen, D., Chessell, I., Humphrey, P., & Belmonte, C. (1997). Nociceptors of the cat and rat cornea are not excited by P2X purinoceptor agonists. *British Journal of Pharmacology - Proceedings Supplement*, *122*, 348.

Dowd, E., McQueen, D. S., Chessell, I. P., & Humphrey, P. P. (1998). P2X receptor-mediated excitation of nociceptive afferents in the normal and arthritic rat knee joint. *British Journal of Pharmacology*, *125*(2), 341–346. https://doi.org/10.1038/sj.bjp.0702080

Dunn, P. M., & Blakeley, A. G. H. (1988). Suramin: A reversible P_2-purinoceptor antagonist in the mouse vas deferens. *British Journal of Pharmacology*, *93*(2), 243–245. https://doi.org/10.1111/j.1476-5381.1988.tb11427.x

Dunn, P. M., Zhong, Y., & Burnstock, G. (2001). P2X receptors in peripheral neurons. *Progress in Neurobiology*, *65*(2), 107–134. https://doi.org/10.1016/s0301-0082(01)00005-3

Eriksson, J., Bongenhielm, U., Kidd, E., Matthews, B., & Fried, K. (1998). Distribution of P2X3 receptors in the rat trigeminal ganglion after inferior alveolar nerve injury. *Neuroscience Letters*, *254*(1), 37–40. https://doi.org/10.1016/s0304-3940(98)00656-9

Fakih, D., Guerrero-Moreno, A., Baudouin, C., Réaux-Le Goazigo, A., & Parsadaniantz, S. M. (2021). Capsazepine decreases corneal pain syndrome in severe dry eye disease. *Journal of Neuroinflammation*, *18*(1), 111. https://doi.org/10.1186/s12974-021-02162-7

Flegel, C., Schöbel, N., Altmüller, J., Becker, C., Tannapfel, A., Hatt, H., & Gisselmann, G. (2015). RNA-Seq analysis of human trigeminal and dorsal root ganglia with a focus on chemoreceptors. *PLoS ONE*, *10*(6), e0128951. https://doi.org/10.1371/journal.pone.0128951

Frank, J. A., Moroni, M., Moshourab, R., Sumser, M., Lewin, G. R., & Trauner, D. (2015). Photoswitchable fatty acids enable optical control of TRPV1. *Nature Communications*, *6*(1), 7118. https://doi.org/10.1038/ncomms8118

Frutos-Rincón, L., Luna, C., Aleixandre-Carrera, F., Velasco, E., Diaz-Tahoces, A., Meseguer, V., Gallar, J., & Acosta, M. C. (2023). The contribution of TRPA1 to corneal thermosensitivity and blink regulation in young and aged mice. *International Journal of Molecular Sciences*, *24*(16), 12620. https://doi.org/10.3390/ijms241612620

González-González, O., Bech, F., Gallar, J., Merayo-Lloves, J., & Belmonte, C. (2017). Functional properties of sensory nerve terminals of the mouse cornea. *Investigative Ophthalmology & Visual Science*, *58*(1), 404–415. https://doi.org/10.1167/iovs.16-20033

Grishin, E. V., Savchenko, G. A., Vassilevski, A. A., Korolkova, Y. V., Boychuk, Y. A., Viatchenko-Karpinski, V. Y., Nadezhdin, K. D., Arseniev, A. S., Pluzhnikov, K. A., Kulyk, V. B., Voitenko, N. V., & Krishtal, O. O. (2010). Novel peptide from spider venom inhibits P2X3 receptors and inflammatory pain. *Annals of Neurology*, *67*(5), 680–683. https://doi.org/10.1002/ana.21949

Hirata, H., & Meng, I. D. (2010). Cold-sensitive corneal afferents respond to a variety of ocular stimuli central to tear production: Implications for dry eye disease. *Investigative Ophthalmology & Visual Science*, *51*(8), 3969–3976. https://doi.org/10.1167/iovs.09-4744

Honore, P., Donnelly-Roberts, D., Namovic, M. T., Hsieh, G., Zhu, C. Z., Mikusa, J. P., Hernandez, G., Zhong, C., Gauvin, D. M., Chandran, P., Harris, R., Medrano, A. P., Carroll, W., Marsh, K., Sullivan, J. P., Faltynek, C. R., & Jarvis, M. F. (2006). A-740003 [*N*-(1-{[(cyanoimino)(5-quinolinylamino) methyl]amino}-2,2-dimethylpropyl)-2-(3,4-dimethoxyphenyl)acetamide], a novel and selective P2X7 receptor antagonist, dose-dependently reduces neuropathic pain in the rat. *Journal of Pharmacology and Experimental Therapeutics*, *319*(3), 1376–1385. https://doi.org/10.1124/jpet.106.111559

Hoyle, C. H. V., Knight, G. E., & Burnstock, G. (1990). Suramin antagonizes responses to P_2-purinoceptor agonists and purinergic nerve stimulation in the guinea-pig urinary bladder and taenia coli. *British Journal of Pharmacology*, *99*(3), 617–621. https://doi.org/10.1111/j.1476-5381.1990.tb12979.x

Inoue, K. (2022). The role of ATP receptors in pain signaling. *Neurochemical Research*, *47*(9), 2454–2468. https://doi.org/10.1007/s11064-021-03516-6

Kabanova, N. V., Vassilevski, A. A., Rogachevskaja, O. A., Bystrova, M. F., Korolkova, Y. V., Pluzhnikov, K. A., Romanov, R. A., Grishin, E. V., & Kolesnikov, S. S. (2012). Modulation of P2X3 receptors by spider toxins. *Biochimica et Biophysica Acta (BBA)*, *1818*(11), 2868–2875. https://doi.org/10.1016/j.bbamem.2012.07.016

Ko, K. W., Rasband, M. N., Meseguer, V., Kramer, R. H., & Golding, N. L. (2016). Serotonin modulates spike probability in the axon initial segment through HCN channels. *Nature Neuroscience*, *19*(6), 823–834. https://doi.org/10.1038/nn.4293

Kovács, I., Luna, C., Quirce, S., Mizerska, K., Callejo, G., Riestra, A., Fernández-Sánchez, L., Meseguer, V. M., Cuenca, N., Merayo-Lloves, J., Acosta, M. C., Gasull, X., Belmonte, C., & Gallar, J. (2016). Abnormal activity of corneal cold thermoreceptors underlies the unpleasant sensations in dry eye disease. *Pain*, *157*(2), 399–417. https://doi.org/10.1097/j.pain.0000000000000455

Landra-Willm, A., Karapurkar, A., Duveau, A., Chassot, A. A., Esnault, L., Callejo, G., Bied, M., Häfner, S., Lesage, F., Wdziekonski, B., Baron, A., Fossat, P., Marsollier, L., Gasull, X., Boué-Grabot, E., Kienzler, M. A., & Sandoz, G. (2023). A photoswitchable inhibitor of TREK channels controls pain in wild-type intact freely moving animals. *Nature Communications*, *14*(1), 1160. https://doi.org/10.1038/s41467-023-36806-4

Lewis, C., Neidhart, S., Holy, C., North, R. A., Buell, G., & Surprenant, A. (1995). Coexpression of $P2X_2$ and $P2X_3$ receptor subunits can account for ATP-gated currents in sensory neurons. *Nature*, *377*(6548), 432–435. https://doi.org/10.1038/377432a0

Lilley, E., Stanford, S. C., Kendall, D. E., Alexander, S. P. H., Cirino, G., Docherty, J. R., George, C. H., Insel, P. A., Izzo, A. A., Ji, Y., Panettieri, R. A., Sobey, C. G., Stefanska, B., Stephens, G., Teixeira, M., & Ahluwalia, A. (2020). ARRIVE 2.0 and the British Journal of Pharmacology: Updated guidance for 2020. *British Journal of Pharmacology*, *177*, 3611–3616. https://doi.org/10.1111/bph.15178

Marfurt, C. F. (1981). The central projections of trigeminal primary afferent neurons in the cat as determined by the tranganglionic transport of horseradish peroxidase. *Journal of Comparative Neurology*, *203*(4), 785–798. https://doi.org/10.1002/cne.902030414

Matthews, B., Li, F., Khakh, B., & Vongsavan, N. (1997). Effects of ATP on sensory receptors in the dental pulp of cats. *Journal of Physiology (London)*, *504*, 128.

Morenilla-Palao, C., Luis, E., Fernández-Peña, C., Quintero, E., Weaver, J. L., Bayliss, D. A., & Viana, F. (2014). Ion channel profile of TRPM8 cold receptors reveals a role of TASK-3 potassium channels in

thermosensation. *Cell Reports*, *8*(5), 1571–1582. https://doi.org/10.1016/j.celrep.2014.08.003

Moulton, E. A., Becerra, L., Rosenthal, P., & Borsook, D. (2012). An approach to localizing corneal pain representation in human primary somatosensory cortex. *PLoS ONE*, *7*(9), e44643. https://doi.org/10.1371/journal.pone.0044643

Mourot, A., Fehrentz, T., Le Feuvre, Y., Smith, C. M., Herold, C., Dalkara, D., Nagy, F., Trauner, D., & Kramer, R. H. (2012). Rapid optical control of nociception with an ion-channel photoswitch. *Nature Methods*, *9*(4), 396–402. https://doi.org/10.1038/nmeth.1897

Mourot, A., Kienzler, M. A., Banghart, M. R., Fehrentz, T., Huber, F. M. E., Stein, M., Kramer, R. H., & Trauner, D. (2011). Tuning photochromic ion channel blockers. *ACS Chemical Neuroscience*, *2*(9), 536–543. https://doi.org/10.1021/cn200037p

Mourot, A., Tochitsky, I., & Kramer, R. H. (2013). Light at the end of the channel: Optical manipulation of intrinsic neuronal excitability with chemical photoswitches. *Frontiers in Molecular Neuroscience*, *6*, 5.

North, R. A. (2004). $P2X_3$ receptors and peripheral pain mechanisms. *The Journal of Physiology*, *554*(2), 301–308. https://doi.org/10.1113/jphysiol.2003.048587

Parra, A., Gonzalez-Gonzalez, O., Gallar, J., & Belmonte, C. (2014). Tear fluid hyperosmolality increases nerve impulse activity of cold thermoreceptor endings of the cornea. *Pain*, *155*(8), 1481–1491. https://doi.org/10.1016/j.pain.2014.04.025

Parra, A., Madrid, R., Echevarria, D., Del Olmo, S., Morenilla-Palao, C., Acosta, M. C., Gallar, J., Dhaka, A., Viana, F., & Belmonte, C. (2010). Ocular surface wetness is regulated by TRPM8-dependent cold thermoreceptors of the cornea. *Nature Medicine*, *16*(12), 1396–1399. https://doi.org/10.1038/nm.2264

Percie du Sert, N., Hurst, V., Ahluwalia, A., Alam, S., Avey, M. T., Baker, M., Browne, W. J., Clark, A., Cuthill, I. C., Dirnagl, U., Emerson, M., Garner, P., Holgate, S. T., Howells, D. W., Karp, N. A., Lazic, S. E., Lidster, K., MacCallum, C. J., Macleod, M., … Würbel, H. (2020). The ARRIVE guidelines 2.0: Updated guidelines for reporting animal research. *PLoS Biology*, *18*(7), e3000410. https://doi.org/10.1371/journal.pbio.3000410

Pozo, M. A., & Cervero, F. (1993). Neurons in the rat spinal trigeminal complex driven by corneal nociceptors: Receptive-field properties and effects of noxious stimulation of the cornea. *Journal of Neurophysiology*, *70*(6), 2370–2378. https://doi.org/10.1152/jn.1993.70.6.2370

Purslow, C., & Wolffsohn, J. (2007). The relation between physical properties of the anterior eye and ocular surface temperature. *Optometry and Vision Science*, *84*(3), 197–201. https://doi.org/10.1097/OPX.0b013e3180339f6e

Quallo, T., Vastani, N., Horridge, E., Gentry, C., Parra, A., Moss, S., Viana, F., Belmonte, C., Andersson, D. A., & Bevan, S. (2015). TRPM8 is a neuronal osmosensor that regulates eye blinking in mice. *Nature Communications*, *6*(1), 7150. https://doi.org/10.1038/ncomms8150

Quirce, S. (2020). Actividad de los nervios sensoriales de la córnea durante la deficiencia lagrimal crónica y su modulación farmacológica. https://dspace.umh.es/

Staikopoulos, V., Sessle, B. J., Furness, J. B., & Jennings, E. A. (2007). Localization of P2X2 and P2X3 receptors in rat trigeminal ganglion neurons. *Neuroscience*, *144*(1), 208–216. https://doi.org/10.1016/j.neuroscience.2006.09.035

Stieber, J., Wieland, K., Stöckl, G., Ludwig, A., & Hofmann, F. (2006). Bradycardic and proarrhythmic properties of sinus node inhibitors. *Molecular Pharmacology*, *69*(4), 1328–1337. https://doi.org/10.1124/mol.105.020701

Takashima, Y., Ma, L., & McKemy, D. D. (2010). The development of peripheral cold neural circuits based on TRPM8 expression. *Neuroscience*, *169*(2), 828–842. https://doi.org/10.1016/j.neuroscience.2010.05.039

Tochitsky, I., Helft, Z., Meseguer, V., Fletcher, R. B., Vessey, K. A., Telias, M., Denlinger, B., Malis, J., Fletcher, E. L., & Kramer, R. H. (2016). How azobenzene photoswitches restore visual responses to the blind retina. *Neuron*, *92*(1), 100–113. https://doi.org/10.1016/j.neuron.2016.08.038

Tochitsky, I., Polosukhina, A., Degtyar, V. E., Gallerani, N., Smith, C. M., Friedman, A., Van Gelder, R. N., Trauner, D., Kaufer, D., & Kramer, R. H. (2014). Restoring visual function to blind mice with a photoswitch that exploits electrophysiological remodeling of retinal ganglion cells. *Neuron*, *81*(4), 800–813. https://doi.org/10.1016/j.neuron.2014.01.003

Vehof, J., Kozareva, D., Hysi, P. G., Harris, J., Nessa, A., Williams, F. K., Bennett, D. L. H., McMahon, S. B., Fahy, S. J., Direk, K., Spector, T. D., & Hammond, C. J. (2013). Relationship between dry eye symptoms and pain sensitivity. *JAMA Ophthalmology*, *131*(10), 1304–1308. https://doi.org/10.1001/jamaophthalmol.2013.4399

Virginio, C., Robertson, G., Surprenant, A., & North, R. A. (1998). Trinitrophenyl-substituted nucleotides are potent antagonists selective for $P2X_1$, $P2X_3$, and heteromeric $P2X_{2/3}$ receptors. *Molecular Pharmacology*, *53*(6), 969–973. https://doi.org/10.1016/S0026-895X(24)13265-8

How to cite this article: Ares-Suárez, D., Iñigo-Portugués, A., Velasco, E., Quirce, S., Aleixandre-Carrera, F., Díaz-Tahoces, A., Acosta, M. C., Lin, W.-C., Kramer, R. H., Belmonte, C., Gallar, J., & Meseguer, V. (2025). Optochemical modulation of corneal cold nerve terminal impulse activity with a photochromic ion channel blocker. *British Journal of Pharmacology*, 1–15. https://doi.org/10.1111/bph.70189